

# A Model for Anesthetic Effects on Cell Membranes

Ofer Kimchi

## Abstract

Ion channels in the plasma membrane are the functional units of neurons and their misregulation by anesthetic compounds is thought to be the proximate cause of the organism-level anesthetic response. However, the mechanism through which general anesthetics affect these channels remains an open question: although many drugs function by binding to receptors in the cell membrane, the variability in compounds that act as anesthetics suggests that they may have a different mode of operation. Recent experiments have shown that anesthetics lower the transition temperature,  $T_C$ , of a liquid-liquid miscibility critical point of Giant Plasma Membrane-derived Vesicles (GPMVs), and further that the magnitude of this effect is well correlated with the potency of the anesthetic. To understand how anesthetics affect  $T_C$ , we developed a simple Ising model for the membrane as a 2D binary liquid. In our model, Ising spins represent membrane lipids; annealed vacancies, which solubilize the two liquid phases, represent anesthetic molecules. We provide theoretical predictions for 1) the change in  $T_C$  of the membrane as a function of the potency-normalized amount of anesthetic in a volume surrounding it and 2) the mole fraction of anesthetic in the membrane at anesthetic dose. We demonstrate that these predictions are in good agreement with results from GPMV assays and synthetic bilayers, respectively.

Ofer Kimchi '16  
Department of Physics  
Program in Applied and Computational Mathematics  
Princeton University  
Advisor: Benjamin Machta  
Second Reader: William Bialek

*This paper represents my own work in accordance with University regulations.*

# 1 Background

The scientific community’s understanding of the function of the cell membrane has undergone major changes in recent years. The lipid membrane is known to be heterogeneous, and regulation of this heterogeneity is essential to proper functionality of the cell in a variety of ways. For example, lipid rafts, organized lipid microdomains in the cell membrane, have been implicated in functions ranging from signal transduction [1] to ion channel regulation [2]. These microdomains have been proposed to arise from the cell membrane’s proximity to a liquid-liquid miscibility critical point,  $T_C$  [3, 4]. Perturbations of the proximity of the membrane to  $T_C$ , such as temperature changes and changes in the cholesterol content of the membrane, affect the function of numerous membrane-bound proteins and ion channels, as shown in both experimental [5, 6, 7, 8] and our own simulation-based [Kimchi and Machta, unpublished results] studies. In fact, it has been hypothesized that anesthetics, whose effect on numerous ligand-gated ion channels is widely acknowledged as the proximate cause of the organism-level anesthetic response [9, 6] (for a countering view, see Ref. [10]), act, at least in part, by perturbing membrane criticality [6]. The motivation for this hypothesis will now be described in detail.

The clinical effects which define general anesthetics are similar across a wide range of anesthetics, and furthermore similar across a range of organisms susceptible to anesthesia [11]. However, the structures of anesthetics are not uniform, with compounds as varied as Xenon [12], propofol [13], and decanol [14] all exhibiting similar clinical properties, though each with different potencies (the higher the potency, the lower concentration of the anesthetic is necessary to achieve anesthetic effects). Moreover, compounds with similar chemical structure often have very different anesthetic properties: for example, n-chain alcohols are anesthetics, but only for  $n < 13$ , and the R(+) stereoisomer of isoflurane is about twice as potent as the S(-) stereoisomer [15, 16]. The variety in the chemical structure of anesthetics, coupled with the large number of receptors affected by anesthetics, have led many to believe anesthetics exert their influence through nonspecific effects, rather than by binding to specific proteins [6, 17].

Many of the hypotheses for non-local anesthetic action center around lipid-mediated effects. These are inspired in a large part by the Meyer-Overton correlation between anesthetic potency and hydrophobicity (measured through the olive oil-gas partition coefficient), which spans over four orders of magnitude in overall concentration and predates the discovery of lipid rafts by nearly a century [18, 19]. The lipid-mediated hypothesis is further strengthened by the observation that anesthesia is reversed at pressures of  $\sim 150$  atm, which are known to affect membrane lipids but are an order of magnitude too small to affect proteins directly [20]. At the same time, theories for non-specific anesthetic action have faced some criticism. It is not clear to what extent the lipid-mediated hypothesis conflicts with evidence in some cases of anesthetics competing with endogenous ligands to bind to proteins, as has been shown by Franks and Lieb in the case of the firefly luciferase protein [21], and the hypothesis is not universally accepted [22]. However, further research has demonstrated that anesthetic inhibition of luciferase is not reversed by high pressures [23, 24] and that anesthetics generally act as allosteric modulators of ion channels rather than by competitive inhibition [25].

Recent research by the Veatch group has suggested that anesthetics exert at least some of their effect by lowering the temperature of the liquid-liquid critical point of the membrane,  $T_C$ . The temperature of GPMVs is naturally tuned to  $\sim 5\%$  above  $T_C$  (which is around  $289K$ ), and a range of anesthetics have been found to decrease  $T_C$  by  $\sim 4K$  at their anesthetic dose, regardless of their respective potencies (Figure 1, reproduced from Ref. [6]). Furthermore, several non-anesthetic compounds structurally similar to these anes-

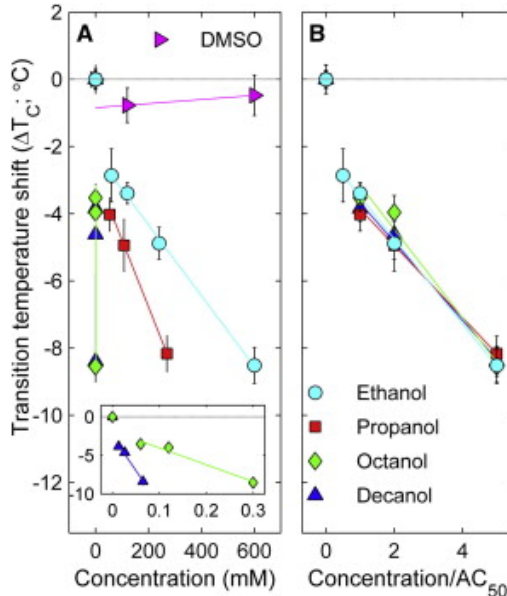


Figure 1: **Effect of Anesthetics on  $T_C$  is Proportional to Anesthetic Potency.** The shift in the critical temperature,  $T_C$ , of GPMVs after the addition of various n-alcohol anesthetics is plotted in (A) as a function of anesthetic concentration, and in (B) as a function of anesthetic concentration normalized by anesthetic potency. The agreement in (B) among various anesthetics with different potencies suggests that anesthetics may exert at least some of their effect by changing critical properties of the cell membrane, and demonstrates that anesthetics' effect on  $T_C$  is a good predictor of anesthetic potency. Non-anesthetic DMSO is used as a control. Figure from Gray *et. al* (2013) [6]. Reproduced with permission.

thetics (and with similar hydrophobic properties) have been found to not affect  $T_C$  [6]. In this way the magnitude of this effect seems to be a better predictor of anesthetic potency than hydrophobicity. However, it is not clear yet how anesthetics may exert this effect on membrane criticality.

To understand how anesthetics affect  $T_C$ , we employ a simple Ising model for the membrane as a 2D liquid. In our model, Ising spins represent membrane lipids, while vacancies, or zero-spins, represent anesthetic molecules. This model is described in Sections 2 and 3. Using Monte Carlo simulations (described in Sections 4 and 5) along with a novel technique for estimating  $T_C$  (Section 6), we provide a theoretical prediction for the change in  $T_C$  of the membrane as a function of the potency-normalized amount of anesthetic in a volume surrounding it, which is demonstrated to be in qualitative agreement with experimental results from GPMV assays, depicted in Fig. 1. Furthermore, our model provides a prediction for the mole fraction of anesthetic in the membrane at anesthetic dose, demonstrated to be in good quantitative agreement with experimental measurements using synthetic bilayers.

## 2 The Ising Model

The Ising Model was originally developed to describe a ferromagnetic system [26]. Despite its applicability to numerous other systems, such as the two dimensional miscibility transition described here, the terminology of the Ising model is based in quantum mechanics. We say that the Ising model describes a collection of spins,  $\{s\}$  each of which can take on one of two values,  $s_i = \pm 1$ . Each spin occupies a point on a lattice which can in principle be of any size, though for simplicity, we choose it to be a square of area  $N^2$  with periodic boundary

conditions, where we set  $N = 256$  throughout our study. For our purposes, the collection of spins represents the (two-dimensional) cell membrane, and each  $s_i$  represents a lipid, which can be either saturated or unsaturated (corresponding to the two values a spin can take).

The Ising model also requires a Hamiltonian, which is a function of a given configuration of spins in the lattice,  $\{s\}$ :

$$\mathcal{H}(\{s\}) = -J \sum_{\langle ij \rangle} s_i s_j \quad (1)$$

where  $\langle ij \rangle$  describes nearest neighbors on the lattice and  $J > 0$  is a constant. Because the notation  $\mathcal{H}(\{s\})$  can get cumbersome, we define a state,  $\mu$ , as a given configuration of spins, and  $E_\mu$  as the energy for this configuration. In a thermal ensemble, the Hamiltonian describes a probability for a given state:

$$P(\mu) \propto e^{-E_\mu/T} \quad (2)$$

where the proportionality constant is defined such that the sum of the probabilities is unity,  $T$  is the temperature of the system, and we have set our units to be such that Boltzmann's constant,  $k_B = 1$ . At low temperatures, the lattice is dominated by either up or down spins because of the energetic favorability of like spins neighboring one another. Biologically, these two phases are known as the liquid-ordered phase ( $l_o$ ) phase, and the liquid disordered ( $l_d$ ) phase [6]. At high temperatures, entropy plays a larger role and the ordering of the spins is mostly random. The temperature separating these regimes is the critical temperature of the model,  $T_C$ , which has been calculated exactly for the two-dimensional square lattice Ising model to be [27]

$$T_C = \frac{2J}{\log(1 + \sqrt{2})} \approx 2.269J \quad (3)$$

Previous experiments have demonstrated that the static behavior of the lipid composition of the cell membrane near  $T_C$  is quantitatively similar to<sup>1</sup> that of the Ising model near its  $T_C$  [28, 29]. This is true even though in the Ising model the fraction of up spins compared to down spins (known as the order parameter) is variable, while in cell membranes the analogous parameter is kept constant, or conserved.

### 3 Adding Anesthetics: The Blume-Capel Model

The Blume-Capel model [30, 31] is an extension of the Ising model which introduces zero-spins, or vacancies<sup>2</sup>. These are spins which take on a value of zero,  $s_i = 0$ , and represent anesthetics in our model. We refer to non-zero spins as ‘‘Ising spins’’. The Blume-Capel model is defined by the Hamiltonian:

$$\mathcal{H} = -J \sum_{\langle ij \rangle} s_i s_j + \mu \sum_i S_i^2. \quad (4)$$

where  $\mu$  is the chemical potential of zero-spins, describing how likely they are to appear on the lattice. As  $\mu \rightarrow -\infty$ , the system becomes equivalent to the Ising model described above. Although  $J$  is set at unity for all simulations, we test the effects of a wide range of  $\mu$ , in order

<sup>1</sup>i.e. they exhibit the same critical exponents

<sup>2</sup>The Blume-Capel model is distinguished from the Blume-Emery-Griffiths, or spin-1 Ising, model by the lack of an interaction term between vacancies in its Hamiltonian [32]. The Blume-Capel model can therefore be thought of as a specific case of the spin-1 Ising model where this interaction term coefficient,  $K$ , is set to zero.

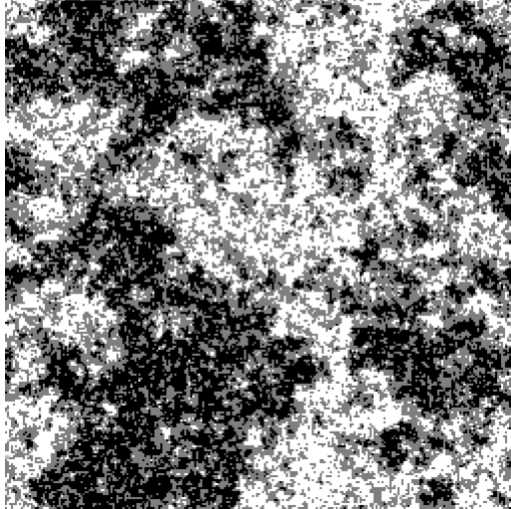


Figure 2: **Vacancies Are Placed on Boundaries of Ising Spins at Equilibrium** Because vacancies can neighbor either type of Ising spin with no energy cost, the energy of the system is generally minimized if they are placed at the boundaries between up and down spins. Gray sites represent vacancies; black and white represent up and down spins, respectively. The simulation was run at  $T = 0.8$  and  $\mu = 1.9$ .

to simulate adding varying concentrations of anesthetics. Experimentally, anesthetics are added to a volume surrounding the cell membrane, and diffuse into the membrane following basic thermodynamic principles; if we approximate anesthetics as an ideal gas, the simulated concentration of anesthetics in the volume surrounding the membrane is proportional to the fugacity,  $f \equiv e^{\mu/T}$ , in our model [33, 34].

Because vacancies can neighbor either type of Ising spin (or other vacancies, for that matter) with no energy cost, the energy of the system is generally minimized if they are placed at the boundaries between up and down spins. A simulation shown in Fig. 2 demonstrates this behavior at equilibrium (gray sites represent vacancies; black and white represent up and down spins, respectively). The simulation was run at  $T = 0.8$  and  $\mu = 1.9$ .

The placement of vacancies on the boundaries of the Ising spins are expected to solubilize the two phases by decreasing the energy of interaction normally present at their boundary. This increased solubility should lower the critical temperature by a degree dependent on the number of vacancies present. Our goal is to determine if the simple model we have defined above is able to qualitatively replicate the experimental data shown in Fig. 1, which would demonstrate that anesthetics may solubilize the  $l_o$  and  $l_d$  phases just as vacancies act as a buffer at the interface of up and down spins. To do so, we find  $T_C$  as a function of  $\mu$  using Monte Carlo simulations of the system at varying values of  $\mu$ . We perform Monte Carlo simulations using stochastic Metropolis and Wolff dynamics, described below, which sample states according to the Boltzmann distribution (Eqn. 2).

## 4 Algorithm for Monte Carlo Simulations: Metropolis Dynamics

The standard Monte Carlo simulations for the Blume-Capel model which we utilize here are Metropolis dynamics which act as follows [35]:

1. Choose a site in the lattice at random.
2. Choose a value (0, +1, or -1) to which to attempt to flip the spin occupying the site.
3. Calculate the change in the energy of the system,  $\Delta E$ , associated with this flip.
4. Flip the spin with a probability as a function of  $\Delta E$ , chosen as to satisfy detailed balance.

We define a sweep to be  $N^2$  repetitions of this procedure, where  $N^2$  is the number of spins on the lattice, such that on average each spin on the lattice attempts to flip once per sweep.

The probability of flipping the spin in the fourth step of the algorithm must be determined as to satisfy two fundamental properties of the system: ergodicity and detailed balance. Ergodicity denotes the property that there is a finite probability of getting from any one configuration of spins to any other, which is satisfied given the random choices of which spin to attempt flipping if the flipping probability is always non-zero. Detailed balance is satisfied if

$$p_\mu P(\mu \rightarrow \nu) = p_\nu P(\nu \rightarrow \mu) \quad (5)$$

where  $P(\mu \rightarrow \nu)$  is the probability of transitioning from state  $\mu$  to state  $\nu$  given that the system is in state  $\mu$ , and  $p_\mu$  is the probability of being in state  $\mu$  in the first place [36]. The latter is given by the Boltzmann probability (Eqn. 2), and using this, we rearrange Eqn. 5 to yield

$$\frac{P(\mu \rightarrow \nu)}{P(\nu \rightarrow \mu)} = \frac{p_\nu}{p_\mu} = e^{-(E_\nu - E_\mu)/T}. \quad (6)$$

In order to satisfy detailed balance, the probabilities of state transitions must therefore be chosen so as to satisfy Eqn. 6.

After a spin to attempt to flip has been selected, i.e. the state  $\nu$  to which to attempt to switch has been specified, the acceptance of the move,  $A(\mu \rightarrow \nu)$  is calculated as a function of the change in energy resulting from the move,  $\Delta E \equiv E_\nu - E_\mu$ . We want the acceptance probabilities to be maximized so that the lattice will spend most of the simulation time changing states instead of rejecting moves:

$$A(\mu \rightarrow \nu) = \begin{cases} e^{-\Delta E/T} & \text{if } \Delta E > 0 \\ 1 & \text{otherwise.} \end{cases} \quad (7)$$

A system which has our method of choosing states to which to attempt to switch, and acceptance probabilities of these state transitions given by Eqn. 7 (known as Metropolis acceptance probabilities) satisfies detailed balance. A detailed proof, along with a derivation of  $A(\mu \rightarrow \nu)$ , is presented in Section A.

## 5 Algorithm for Monte Carlo Simulations: Wolff Dynamics

The Metropolis algorithm is very slow to equilibrate near  $T_C$  due to a process called “critical slowing-down”. A quantitative measure of this slowing down is given by  $\tau$ , the correlation time of the system, or the typical timescale over which the system reaches an independent state. For  $T \sim T_C$ ,  $\tau$  scales with the size of the system  $N^2$  as  $\tau \sim N^{2z}$  where  $z$  is the dynamic critical exponent [36]. For the Metropolis algorithm,  $z \approx 2$ , meaning that the computation time it takes to run each sweep goes as  $N^4$  [36]. Since simulations of larger systems are less

susceptible to error, we set  $N = 256$ ; this system would take an unreasonably long time to equilibrate using the Metropolis algorithm.

Qualitatively, critical slowing down can be explained thus: as temperature is lowered from infinity, energetic considerations begin to play more of a role compared to entropic, and the average range over which spins are correlated with one another – the correlation length  $\xi$  – increases. As the correlation length increases, groups of the same spin begin to cluster together, forming so-called “domains”, which grow in size as the temperature is lowered. If the Metropolis algorithm samples a spin from the middle of one of these domains, the probability of flipping it is extremely low, and even if this spin is flipped, it will probably be flipped back the next time it is selected. This represents an extraordinary amount of wasted computation time.

There are several algorithms that get around the issue of critical slowing down – and even experience critical speeding-up – by flipping clusters of spins (which all point in the same direction) at a time. The fastest is known as the Wolff algorithm [37, 38] which has a dynamic exponent of  $z \approx 1/4$  [38, 36]. The Wolff algorithm proceeds as follows:

1. Choose a site in the lattice at random, and unless it is a zero-spin, use it as a seed to initialize a cluster. If it is a zero spin, pick a new site.
2. Check each of its neighbors, and if they point in the same direction as the seed spin, add them to the cluster with probability  $P_{Wolff} = 1 - e^{-2/T}$  (this choice of probabilities is motivated in Section B).
3. Repeat step 2 for each spin added to the cluster, until the addition of the neighbors of all the spins in the cluster has been attempted (though the addition of some neighbors may have been attempted more than once if they neighbor multiple spins in the cluster).
4. If the seed spin has value  $+1$  flip all spins in the cluster to  $-1$ , and vice versa.

The size of the final cluster that is flipped thus depends only on the temperature of the system. An example of a cluster flip using the Wolff algorithm is presented in Fig. 3, reproduced from Ref. [39]. The top-left panel shows the lattice before the cluster flip. The spins which are part of the cluster which was created are shaded in the top-right panel, while the cluster is shown in isolation from the rest of the lattice in the bottom-right. The lattice after the flip is pictured in the bottom-left. The simulation used was performed with parameter values  $N = 100$ ,  $T = 0.97 T_C$ ,  $\mu \rightarrow -\infty$ .

A proof that the Wolff algorithm obeys detailed balance is presented in Section B. However, since the Wolff algorithm is only able to act on spins with value  $\pm 1$ , it is insufficient for ergodicity in our case [40]. With this in mind, we alternate Wolff sweeps with Metropolis sweeps. For the duration of each Wolff sweep, the vacancies are kept immobile (or “quenched”), while they are free to flip (or “annealed”) during the Metropolis sweeps. For detailed balance to be maintained with this approach, a Wolff sweep must be defined by the number of clusters it flips, rather than by the number of spins flipped (which is how a Metropolis sweep is defined) [41]. It is not clear how many clusters should be flipped each Wolff sweep to achieve an optimal equilibration rate, so we use a programming approach which keeps track of the amount of time it takes to perform each Wolff and Metropolis sweep: if the amount of time spent on the Wolff sweep exceeds the time spent on Metropolis, the number of clusters to flip during the next Wolff sweep is increased, and vice versa.

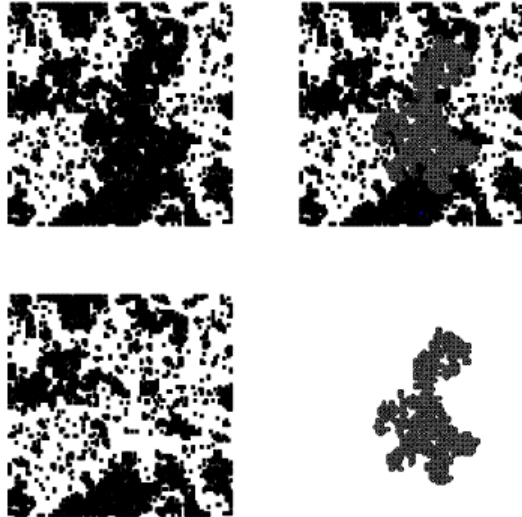


Figure 3: **A Sample Wolff Cluster Flip** Top left: initial lattice configuration. Top right, bottom right: cluster created by Wolff algorithm. Bottom left: lattice configuration after cluster flip. Simulation run at  $N = 100$ ,  $T = 0.97 T_C$ ,  $\mu \rightarrow -\infty$ . Figure reproduced from Ref. [39].

## 6 Determining the Critical Temperature

We have already defined the model to be used, as well as the algorithms we use to equilibrate the lattice. Our goal is to determine  $T_C$  as a function of the fugacity at  $T_C$ ,  $e^{\mu/T_C}$ . Previous studies have determined a fast method for determining  $T_C$  on an Ising lattice with no vacancies: the invaded cluster algorithm [42, 43]. This algorithm finds the critical temperature by continuously adjusting the temperature at which cluster-flipping Monte Carlo moves are performed, using a negative-feedback loop, until it reaches the minimum temperature at which a cluster percolates, or reaches from one end of the lattice to the other. This property of percolating clusters is a property of lattices with  $T \leq T_C$ , and is therefore used to define  $T_C$  using the invaded cluster approach. For our purposes, however, the invaded cluster algorithm is not useful since it is not clear to what extent percolating clusters are a property of the proximity of the system to  $T_C$  in the Blume-Capel model.

Our approach for finding  $T_C$  has much in common with the invaded cluster approach. We start the simulation for a given  $\mu$  with all spins pointing down, at a temperature we know is below  $T_C$ . We then perform alternating Wolff and Metropolis sweeps until the lattice has reached equilibrium, and check if the lattice has reached  $T_C$  in a manner we will explain shortly. If it hasn't, we increase the temperature by a fixed amount  $\Delta T$  and allow the lattice to equilibrate again, repeating the process until  $T_C$  has been found. Given that the Wolff and Metropolis algorithms have different correlation times, it is not immediately clear how many sweeps are necessary to equilibrate the lattice; we found that 1000 rounds of alternating Wolff and Metropolis sweeps were sufficient for our purposes to reach equilibrium, though employing longer simulations would likely increase the accuracy of our results. Unless specified otherwise, we use  $\Delta T = 0.01$  for all  $\mu$ .

The criterion for  $T_C$  we use is based on the fact that for all temperatures below  $T_C$ , the lattice has the property that most of the Ising spins will be either up or down. Wolff moves will likely change which spin is in excess, but if the Metropolis phase begins with one Ising spin outnumbering the other for  $T < T_C$ , this property is not expected to change throughout the Metropolis phase. Therefore, we find  $T_C$  as the minimum temperature at which, during

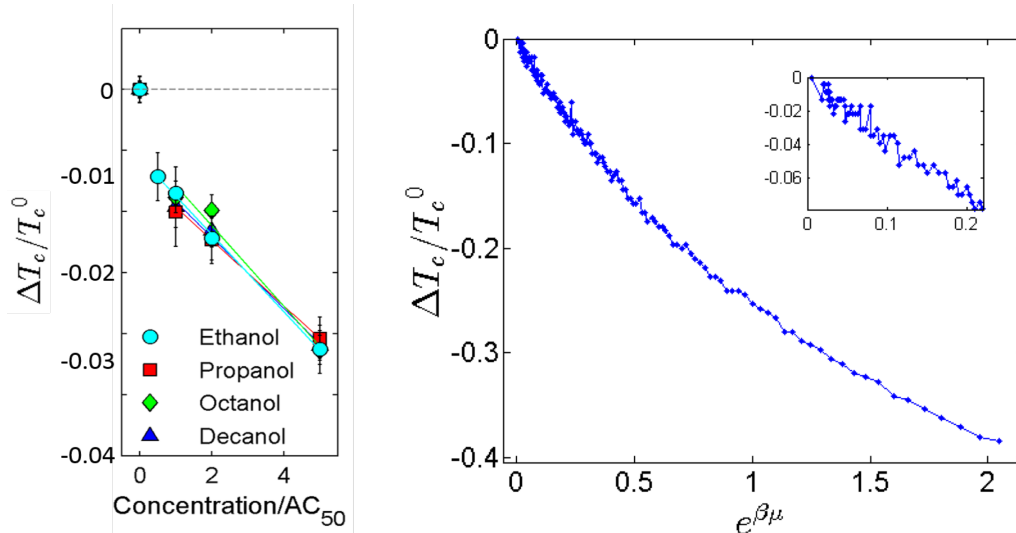


Figure 4: **Change in  $T_C$  as a Function of Fugacity** Left: experimental results for the unitless change in  $T_C$  of the cell membrane ( $\Delta T_C/T_C^0$ , where  $T_C^0$  is the critical temperature of the cell membrane with no anesthetics added) as a function of the potency-normalized amount of anesthetic in a volume surrounding the membrane. Calculated using data from Ref. [6]. Right: Simulation results for the unitless change in  $T_C$  of the lattice as a function of the fugacity of the system are in good qualitative agreement with experimental results. Inset: Our estimation of  $T_C$  is inherently noisy, leading us to examine a wider range of values of  $\Delta T_C$  than probed experimentally.

a Metropolis sweep, the numbers of up and down spins in the lattice are equal.

There are two reference points which we used to check the accuracy of our method against established results. First, for  $\mu \rightarrow -\infty$ , our model approaches the Ising model solved exactly by Onsager to find  $T_C \approx 2.269$ ; our method, using  $\Delta T = 0.001$  and  $\mu = -1000$ , finds  $T_C = 2.279$ , an error of  $< 1\%$ . Second, the Blume-Capel model contains a tricritical point which marks the boundary between first-order and continuous phase transitions in the model. Established values in the literature have placed the tricritical point at  $\mu \approx 1.9658$ ,  $T \approx 0.6086$  [44, 45]; we found, using  $\Delta T = 10^{-5}$ , that for  $\mu = 1.9658$  the critical temperature is at  $T = 0.62858$ . This latter measurement is indicative of a greater imprecision in our method compared to more rigorous methods (such as finite-size scaling) though this level of precision is sufficient to determine qualitative agreement or disagreement between our model and experiment.

## 7 Results and Discussion

Using the method described in Section 6, we calculated the critical temperature for range of systems with different values of  $\mu$ . We used values of  $\mu$  ranging from  $\mu = 1.95$  (near tricriticality) to  $\mu = -9.0$ . Increments of  $\Delta\mu = 0.05$  were used for  $\mu$  greater than  $-3.7$ , and increments of  $\Delta\mu = 0.1$  were used for the smaller values of  $\mu$ , resulting in a total of 167 different values of  $\mu$  tested. For each  $\mu$ , we examined the change in critical temperature due to the introduction of vacancies into the model:  $\Delta T_C/T_C^0$ , where  $T_C^0$  is the critical temperature defined in Eqn. 3 and  $\Delta T_C$  is the difference between the critical temperature of the system at  $\mu$  and  $T_C^0$ .

The results of our simulations are plotted on the right in Fig. 4 as a function of the fugacity of the system,  $e^{\beta\mu} \equiv e^{\mu/T_C}$ . These results are compared to the experimental results

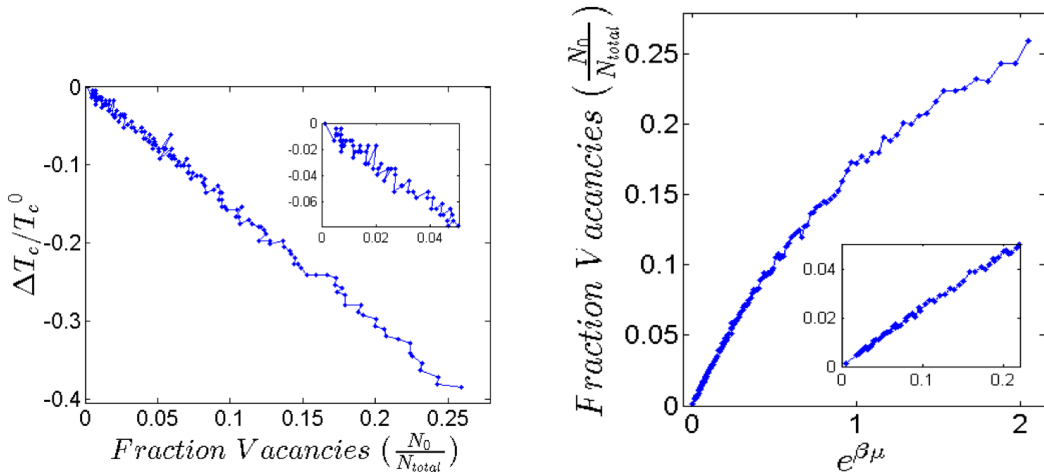


Figure 5: **Mole Fraction of Anesthetics in the Membrane at Anesthetic Dose** Left: our results suggest that  $\Delta T_C$  is expected to scale linearly with the mole fraction of anesthetics in the membrane, for which the proxy in our model is the fraction of the lattice composed of zero spins at  $T_C$ . Right: the nonlinearity observed in Fig. 4 is a result of the nonlinear relationship between the mole fraction of anesthetics in the membrane and the concentration of anesthetics in a volume surrounding it.

of Gray *et al.* (Fig. 4, left) [6]. The noise in our results (Fig. 4, right, inset) leads us to consider a much wider range of values of  $\mu$ , and therefore, of changes in  $T_C$ , than examined experimentally. Furthermore, because the proportionality constant relating the experimental potency-normalized concentration of anesthetics and the fugacity in the model is unknown, direct quantitative comparison of our results to experiment is not possible; however, the curvature of our results is in good qualitative agreement with experimental results.

Several experiments have measured the Mole Fraction of Anesthetics in the membrane at anesthetic dose (MFA) [33, 46], though no experiments have yet examined how  $\Delta T_C$  scales with the MFA. By examining the fraction of the lattice comprised of zero spins at  $T_C$  ( $N_0/N_{total}$ , where  $N_0$  is the number of zero spins in the lattice at  $T_C$  and  $N_{total} = N^2$  is the total number of spins in the lattice), we find that our model predicts a linear relationship between the MFA and  $\Delta T_C$  (Fig. 5, left). The nonlinearity observed in Fig. 4 is therefore due to the nonlinear relationship between the fugacity and the fraction of vacancies in the membrane at  $T_C$  (Fig. 5, right).

Our model makes a quantitative prediction for the mole fraction of anesthetics in the membrane at anesthetic dose, which was determined by Gray *et al.* to be the dose which decreases  $T_C$  such that  $\Delta T_C/T_C^0 \approx 4/296$  [6]. Using the results shown in Fig. 5 (left), we find that at anesthetic dose,

$$0.0125 < \frac{N_0}{N_{total}} < 0.0172. \quad (8)$$

This prediction agrees well with the results of various experimental studies that have used synthetic bilayers to examine the mole fraction of anesthetics in the membrane at anesthetic dose, and found that  $0.011 < MFA < 0.045$  [46, 47].

## 8 Conclusions

Motivated by recent experiments by Gray *et al.* which suggest anesthetics may exert their functional effect by perturbing critical properties of cell membranes, we have developed a simple model for examining the effects of anesthetics on the critical temperature of cell membranes. We employ the 2D Blume-Capel model, modeling membrane lipids as Ising spins and anesthetics as vacancies. Using Monte Carlo simulations of the Blume-Capel model and employing a novel technique for estimating  $T_C$ , we show that our model exhibits good agreement with experimental measurements. Our model qualitatively replicates the experimentally-observed nonlinear relationship between the change in  $T_C$  of the cell membrane and the potency-normalized concentration of anesthetics in a volume surrounding it (Fig. 4). Furthermore, our model makes a quantitative prediction of the mole fraction of anesthetics at anesthetic dose, which is in excellent agreement with experimental results. Thus, our results suggest that anesthetics solubilize the two liquid phases of the cell membrane ( $l_o$  and  $l_d$ ) just as vacancies solubilize the two phases of the Ising model.

## A Appendix: The Metropolis Acceptance Probability

Here we describe the steps taken to get to Eqn. 7. We start from Eqn. 6. In principle, any set of probabilities  $P(\mu \rightarrow \nu)$  will work, as long as they satisfy Eqn. 6, and have the characteristics of a probability distribution (i.e.  $0 \leq P(\mu \rightarrow \nu) \leq 1$  and  $\sum_{\nu} P(\mu \rightarrow \nu) = 1$ ). However, depending on the probability, the simulation will take different times to run. Minimizing the run time of the simulation implies maximizing the probabilities  $P(\mu \rightarrow \nu)$ . To simplify our description of the solution we choose, let us write them in another form, where we take advantage of our simulation algorithm. Our algorithm, as described above, first picks a state to which to attempt to switch,  $\nu$ , which differs from the current state,  $\mu$ , by a single exchange of spins. We denote the probability of choosing a given state as  $g(\mu \rightarrow \nu)$ . Then, the algorithm accepts this change of state with some probability,  $A(\mu \rightarrow \nu)$ . Therefore, we can write

$$P(\mu \rightarrow \nu) = g(\mu \rightarrow \nu)A(\mu \rightarrow \nu) \quad (9)$$

As described above, the only state to which we attempt to switch in our algorithm is one which differs from our current state only by an exchange of spins. Furthermore, we choose from among these states randomly, with no weighting of states. In other terms, for each iteration of our algorithm, given the system is currently in a state  $\mu$ , the algorithm will select a state  $\nu$  to which to switch with the following probability:

$$g(\mu \rightarrow \nu) = \begin{cases} \text{constant} & \text{if } \nu \text{ differs from } \mu \text{ by only a spin exchange} \\ 0 & \text{otherwise.} \end{cases} \quad (10)$$

For practical purposes, the value of the constant is not important. We can now write Eqn. 6 for our algorithm as

$$\frac{P(\mu \rightarrow \nu)}{P(\nu \rightarrow \mu)} = \frac{A(\mu \rightarrow \nu)}{A(\nu \rightarrow \mu)} = e^{-(E_{\nu} - E_{\mu})/T} \quad (11)$$

As we have suggested earlier, we want the acceptance probabilities to be maximized so that the lattice will spend most of the simulation time changing states instead of rejecting moves. We do this by setting the larger of the acceptance probabilities to unity and the smaller to be such that Eqn. 11 is satisfied. This acceptance probability is named after N. Metropolis [35]:

$$A(\mu \rightarrow \nu) = \begin{cases} e^{-\Delta E/T} & \text{if } \Delta E > 0 \\ 1 & \text{otherwise.} \end{cases} \quad (12)$$

where as before,  $\Delta E \equiv E_\nu - E_\mu$ .

## B Appendix: $P_{Wolff}$ and the Wolff Acceptance Probability

Here we describe the motivation for the choice of  $P_{Wolff}$ , or the probability of adding similarly-oriented spins to the cluster, given in the text. To review, the Wolff algorithm picks a spin at random and uses it to initialize a cluster. It then checks each of the neighbors of the seed spin and if they point in the same direction as the seed, adds them to the cluster with probability  $P_{Wolff}$ . The neighbors of each of *these* spins is then checked, and the process is repeated, until the addition of the neighbors of all the spins in the cluster has been attempted. Then, the entire cluster is flipped with some acceptance probability  $A$ . Our analysis here closely follows Newman and Barkema's [36].

Consider a Wolff move which takes the system from state  $\mu$  to state  $\nu$ , and consider also the reverse move, from  $\nu$  to  $\mu$ . The probability of choosing the specific cluster that is flipped in the transition between the two states depends on the probabilities of: 1) adding to the cluster all of the similarly-oriented spins flipped in the transition between the states, and 2) *not* adding to the cluster those spins not flipped in the same transition. The first probability is the same in the forward and reverse moves, because the probability of adding any given similarly-oriented spin to the cluster is given by  $P_{Wolff}$ . However, because the edges of the cluster in general border different numbers of similarly- and oppositely-oriented spins, the second probability is different between the forward and reverse moves. Therefore, the probability of creating the same cluster in the forward move,  $g(\mu \rightarrow \nu)$  is not the same as that for the reverse move,  $g(\nu \rightarrow \mu)$ . In fact, their ratio is dependent on the number of spins not added to the cluster in the forward move,  $m$ , and in the reverse move,  $n$ :

$$\frac{g(\mu \rightarrow \nu)}{g(\nu \rightarrow \mu)} = (1 - P_{Wolff})^{m-n}. \quad (13)$$

In order for the system to obey detailed balance, we must therefore assert that

$$\frac{A(\mu \rightarrow \nu)}{A(\nu \rightarrow \mu)} (1 - P_{Wolff})^{m-n} = e^{-(E_\nu - E_\mu)/T}. \quad (14)$$

We recognize that the difference  $E_\nu - E_\mu$  also depends on the difference between  $m$  and  $n$ :

$$E_\nu - E_\mu = 2(m - n), \quad (15)$$

regardless of whether zero-spins are present in the lattice.

Substituting into Eqn. 14, we find that:

$$\frac{A(\mu \rightarrow \nu)}{A(\nu \rightarrow \mu)} = [e^{2/T} (1 - P_{Wolff})]^{m-n}. \quad (16)$$

It appears that the acceptance ratios must therefore depend on the specifics of the move (namely,  $m$  and  $n$ ). However, we notice that for a specific choice of  $P_{Wolff}$ , we can let the acceptance ratios for both moves be unity, which is the maximum value they can take. Thus, we set

$$P_{Wolff} = 1 - e^{-2/T}, \quad (17)$$

and

$$A(\mu \rightarrow \nu) = A(\nu \rightarrow \mu) = 1. \quad (18)$$

## References

- [1] K. Simons and D. Toomre, *Nature Reviews Molecular Cell Biology* **1**, 31 (2000).
- [2] C. Dart, *The Journal of Physiology* **588**, 3169 (2010).
- [3] A. Rietveld and K. Simons, *Biochimica et Biophysica Acta (BBA) - Reviews on Biomembranes* **1376**, 467 (1998).
- [4] S. L. Veatch, *Seminars in Cell & Developmental Biology* **18**, 573 (2007), Membrane Lipid Microdomains: Roles in Signalling and Disease and 3D Chromatin Structure Inside the Cell Nucleus.
- [5] R. E. Wachtel, *Journal of Pharmacology and Experimental Therapeutics* **274**, 1355 (1995).
- [6] E. Gray, J. Karstlake, B. Machta, and S. Veatch, *Biophysical Journal* **105**, 2751 (2013).
- [7] S. Rankin, G. Addona, M. Kloczewiak, B. Bugge, and K. Miller, *Biophysical Journal* **73**, 2446 (1997).
- [8] M. F. Brown, *Chemistry and Physics of Lipids* **73**, 159 (1994), Special Issue Functional Dynamics of Lipids in Biomembranes.
- [9] N. Franks and W. Lieb, *Nature* **367**, 607 (1994).
- [10] L. D. Mosgaard and T. Heimburg, *Accounts of Chemical Research* **46**, 2966 (2013), PMID: 23902303.
- [11] J. A. Humphrey et al., *Current Biology* **17**, 624 (2007).
- [12] S. C. Cullen and E. G. Gross, *Science* **113**, 580 (1951).
- [13] P. H. M. Tonner, D. M. Poppers, and K. W. P. Miller, *Anesthesiology* **77**, 926 (1992).
- [14] M. J. Pringle, K. B. Brown, and K. W. Miller, *Molecular Pharmacology* **19**, 49 (1981).
- [15] K. H. Meyer and H. Hemmi, *Biochem. Z* **277**, 39 (1935).
- [16] N. Franks and W. Lieb, *Science* **254**, 427 (1991).
- [17] R. S. Cantor, *The Journal of Physical Chemistry B* **101**, 1723 (1997).
- [18] H. Meyer, *Archiv far experimentelle Pathologie und Pharmakologie* **42**, 109 (1899).
- [19] C. Overton, *Studien ber die Narkose zugleich ein Beitrag zur allgemeinen Pharmakologie*, Gustav Fischer, Jena, Switzerland., 1901.
- [20] D. B. Mountcastle, R. L. Biltonen, and M. J. Halsey, *Proceedings of the National Academy of Sciences* **75**, 4906 (1978).
- [21] N. Franks and W. Lieb, *Nature* **310**, 599 (1984).

- [22] N. Franks and W. Lieb, *Nature* **300**, 487 (1982).
- [23] G. Moss, W. Lieb, and N. Franks, *Biophysical Journal* **60**, 1309 (1991).
- [24] I. Ueda, H. Minami, H. Matsuki, and T. Inoue, *Biophysical Journal* **76**, 478 (1999).
- [25] S. J. Mihic et al., *Nature* **389**, 385 (1997).
- [26] E. Ising, *Zeitschrift fur Physik* **31**, 253 (1925).
- [27] L. Onsager, *Phys. Rev.* **65**, 117 (1944).
- [28] A. R. Honerkamp-Smith et al., *Biophysical Journal* **95**, 236 (2008).
- [29] S. L. Veatch et al., *ACS Chemical Biology* **3**, 287 (2008), PMID: 18484709.
- [30] M. Blume, *Phys. Rev.* **141**, 517 (1966).
- [31] H. Capel, *Physics Letters* **23**, 327 (1966).
- [32] M. Blume, V. J. Emery, and R. B. Griffiths, *Phys. Rev. A* **4**, 1071 (1971).
- [33] K. W. Miller, *Int Rev Neurobiol.* **27**, 1 (1985).
- [34] C. Kittel and H. Kroemer, *Thermal Physics*, W. H. Freeman, 1980.
- [35] N. Metropolis, A. Rosenbluth, M. Rosenbluth, A. Teller, and E. Teller, *The Journal of Chemical Physics* **21**, 1087 (1953).
- [36] M. E. J. Newman and G. T. Barkema, *Monte Carlo methods in statistical physics*, Clarendon Press, Oxford, 1999.
- [37] U. Wolff, *Phys. Rev. Lett.* **62**, 361 (1989).
- [38] C. F. Baillie and P. D. Coddington, *Phys. Rev. B* **43**, 10617 (1991).
- [39] W. Janke, Monte carlo simulations of spin systems, in *Computational Physics*, edited by K. Hoffmann and M. Schreiber, pages 10–43, Springer Berlin Heidelberg, 1996.
- [40] Y. Deng, W. Guo, and H. W. J. Blöte, *Phys. Rev. E* **72**, 016101 (2005).
- [41] B. B. Machta, *Criticality in Cellular Membranes and the Information Geometry of Simple Models*, PhD thesis, Cornell, 2013.
- [42] J. Machta, Y. S. Choi, A. Lucke, T. Schweizer, and L. V. Chayes, *Phys. Rev. Lett.* **75**, 2792 (1995).
- [43] J. Machta, Y. S. Choi, A. Lucke, T. Schweizer, and L. M. Chayes, *Phys. Rev. E* **54**, 1332 (1996).
- [44] X. Qian, Y. Deng, and H. W. J. Blöte, *Phys. Rev. E* **72**, 056132 (2005).
- [45] P. D. Beale, *Phys. Rev. B* **33**, 1717 (1986).
- [46] A. S. Janoff, M. J. Pringle, and K. W. Miller, *Biochimica et Biophysica Acta* **649**, 125 (1981).
- [47] N. Kučerka, S. Tristram-Nagle, and J. F. Nagle, *J. Membrane Biol.* **208**, 193 (2005).